

This is an Open Access document downloaded from ORCA, Cardiff University's institutional repository: <https://orca.cardiff.ac.uk/id/eprint/123737/>

This is the author's version of a work that was submitted to / accepted for publication.

Citation for final published version:

Stenvall, C.A., Fagereng, Å. and Diener, J.F.A. 2019. Weaker than weakest: on the strength of shear zones. *Geophysical Research Letters* 46 (13) , pp. 7404-7413. 10.1029/2019GL083388

Publishers page: <http://dx.doi.org/10.1029/2019GL083388>

Please note:

Changes made as a result of publishing processes such as copy-editing, formatting and page numbers may not be reflected in this version. For the definitive version of this publication, please refer to the published source. You are advised to consult the publisher's version if you wish to cite this paper.

This version is being made available in accordance with publisher policies. See <http://orca.cf.ac.uk/policies.html> for usage policies. Copyright and moral rights for publications made available in ORCA are retained by the copyright holders.



Weaker than weakest: on the strength of shear zones

C. A. Stenvall¹, Å. Fagereng^{1,2}, J. F. A. Diener²

¹School of Earth & Ocean Sciences, Cardiff University, Wales, United Kingdom

²Department of Geological Sciences, University of Cape Town, Private Bag X3, Rondebosch 7701, South Africa

Key Points:

- Decreasing grain size with increasing strain creates favourable conditions for grain size sensitive creep in mid-crustal shear zones
- With increasing strain, weak interconnected phyllosilicate networks can break down and be supplanted by weaker fine-grained polyphase mixtures
- Grain size sensitive creep in fine-grained polyphase mixtures may govern the rheology of the mid-lower continental crust

Abstract

Thin, laterally continuous ultramylonites within kilometer-scale ductile shear zones may control mid-lower crustal strength where deformation is localised. Interconnected phyllosilicate networks are commonly suggested to be the weakest geometry a shear zone can reach, yet fine-grained polyphase mixtures are commonly found in the cores of high strain zones. We study a continental strike-slip shear zone which deformed granulite facies quartzofeldspathic migmatitic gneisses at retrograde amphibolite- to greenschist facies conditions. A brittle feldspar framework and interconnected phyllosilicate networks control the strength of the lower strain protomylonites and mylonites respectively, whereas the ultramylonites comprise a fine-grained mixture of the host rock minerals. The localisation of strain in ultramylonites demonstrates how fine-grained polyphase mixtures can be weaker than, and supersede, interconnected phyllosilicate networks with increasing shear strain. This contradicts the common assumption that interconnected layers of phyllosilicates is the weakest state a shear zone can reach.

1 Introduction

For nearly a century it has been agreed that a hard outer shell encompasses Earth, but the strength of the mid- to lower crust is still debated (Bürgmann & Dresen, 2008). Strength profiles for the continental crust are primarily based on laboratory experiments on quartz and feldspar at conditions favouring dislocation creep (Kohlstedt et al., 1995). Deformation is, however, readily concentrated into localised high strain zones within this quartzofeldspathic crust (e.g. Kirby, 1985; Ingleby & Wright, 2017; Fagereng & Biggs, 2018). These high strain zones exert a critical control on mid- to lower crustal strength, and study of their internal geometry, composition, and microstructure is a means of exploring mechanisms of strain localisation and the consequent controls on lower crustal rheology.

An interconnected network of weak components is a commonly invoked end member weak state for a polyphase rock, with as little as 10 vol.% of relatively weak material potentially sufficient to govern bulk rheology (Handy, 1994). This is not only true for rocks at the centimetre scale (e.g. Hunter et al., 2016), but also for entire shear zones at the kilometre scale, where strain may be accommodated in heterogeneously distributed, thin, high strain zones localised within broader mylonites (e.g. Carreras, 2001). Regardless of geometry, strain localisation does not occur without a relative weakness, where

strength at a given pressure (P), temperature (T), and strain rate is not only a function of mineralogy, but also the dominant deformation mechanism (Knipe, 1989). A switch in deformation mechanism can therefore affect rock strength at least as much as lithological variations.

Phyllosilicates are commonly considered to be the weakest phase in continental rocks (Kronenberg et al., 1990) and interconnected layers of phyllosilicates are therefore commonly suggested as the weakest end-member shear zone geometry (Handy, 1994; Montési, 2013; Shea & Kronenberg, 1993). Once phyllosilicates have been reorganised and interconnected weak layers have been established, continued weakening may nevertheless require an increase in phyllosilicate content, requiring mass transfer to facilitate the compositional changes. Grain size reduction, on the other hand, can induce weakening by facilitating a change in the active deformation mechanisms (Kirby, 1985; Rutter & Brodie, 1988; Viegas et al., 2016). This form of weakening can be isochemical, with no need for special conditions and may hence be more generally applicable. It is widely accepted that fine-grained mixtures can be weak, with grain size sensitive creep in fine-grained polyphase mixtures having been previously shown to operate in the most highly strained parts of shear zones, both in laboratory experiments (e.g. Stünitz & Tullis, 2001) and natural examples (e.g. Fliervoet et al., 1997). However, the processes forming these fine-grained mixtures is still an area of active research (Kilian et al., 2011; Czaplińska et al., 2015; Cross & Skemer, 2017).

Existing studies on the weakening effects of grain size reduction typically consider granitic fine-grained polyphase mixtures against their less deformed equivalents with larger grain sizes. However, in this study, we describe a natural example where interconnected phyllosilicate networks in a mylonite are disaggregated within a weaker fine-grained polyphase mixture, ultimately leading to further strain localisation and the formation of ultramylonites. We thereby demonstrate that fine-grained polyphase mixtures are even weaker than the interconnected phyllosilicate layers commonly thought to be the weakest geometry a shear zone can achieve, and that such mixtures can disaggregate and supplant interconnected phyllosilicate networks with increasing shear strain.

2 Geological setting and outcrop description

The studied rocks are from the continental strike-slip Kuckaus Mylonite Zone (KMZ) in Namibia (Rennie et al., 2013). The KMZ is a sub-vertical, NW-SE striking, ~ 2 km wide dextral shear zone, exposed along strike for ~ 145 km in south-western Namibia (Jackson, 1976; Rennie et al., 2013). The KMZ is part of the Marshall Rocks-Pofadder shear zone system, which extends for 550 km across Namibia and South Africa in rocks of the Namaqua Metamorphic Complex (Miller & Becker, 2008).

The KMZ is localised in 1250-1100 Ma orthogneisses of the Aus Domain. To the NE of the KMZ, the Tsirub Gneiss comprises garnet-bearing tonalitic to granodioritic augen gneiss, whereas biotite gneisses and coarse grained leucogranites, composed of megacrystic K-feldspar and quartz, with minor biotite and garnet, occur to the SW. Both orthogneisses experienced the same high-grade granulite facies peak metamorphism (550 MPa, 825 °C) and partial migmatitisation during the late Namaqua orogeny at 1065-1045 Ma (Diener et al., 2013), whereas the leucogranites were emplaced after peak metamorphism (Rennie et al., 2013).

Deformation in the KMZ took place c. 40 Ma after granulite facies peak metamorphism under retrograde mid-crustal amphibolite- to greenschist facies conditions (420-270 MPa, 480-450 °C; Diener et al., 2016). Shearing was heterogeneously distributed over a < 2 km wide zone that developed a subvertical mylonitic fabric and subhorizontal lineation. The mylonitic fabric is poorly developed within coarse grained leucogranite and migmatite lozenges, whereas more intense fabrics occur in 10s of cm wide ultramylonite zones that wrap around these lower strain rocks. The ultramylonites are steeply dipping, subparallel to the shear zone margins and distinguished from their wall rocks by finer grain size but no change in mineralogy. Here, we focus on one representative high strain zone, to describe patterns of strain localisation.

The following observations are from three samples of granitic composition covering the strain gradient from protomylonite to ultramylonite in a high strain zone localised between a pre-mylonitic leucogranite body and the Tsirub Gneiss (026°48'32.4'' S, 015°58' 04.3'' E; Figures 1 and S1). The granitic side of the local high strain zone was chosen for its simpler mineralogy and, as the granite was emplaced after peak granulite facies metamorphism, its lack of pre-mylonitic fabrics. Here, the mylonitic foliation dips $> 70^\circ$ to the NE, with a lineation plunging $< 10^\circ$ to the SE. The mylonite zone has ir-

regular boundaries but is approximately 6 m wide, with up to 50 cm thick ultramylonite at its core. The transition from mylonite to ultramylonite occurs over a few cms (Figure 1a).

3 Microstructural development

The protomylonite is similar to the granite protolith in mineralogy and comprises 55% feldspar (K-feldspar > plagioclase), 30% quartz, 10% phyllosilicates (mixture of biotite and muscovite) and the remaining 5% are accessory minerals including apatite, zircon and rutile. The mineral proportions for all mylonites are semi-quantitative and based on electron backscatter diffraction (EBSD), scanning electron microscopy (SEM) backscattered electron (BSE) images and optical microscopy, whereas the grain sizes were obtained by EBSD. The microstructure is dominated by subrounded feldspar porphyroclasts, with quartz occupying interstitial spaces. Monomineralic quartz ribbons define the mylonitic foliation in conjunction with aligned but disconnected, fine-grained (50 μm) phyllosilicates (Figure 1b). Quartz was recrystallised during mylonitization to a distinctly smaller grain size than in undeformed equivalents. Quartz grain size ranges from a few μm where pinned between feldspar porphyroclasts to > 100 μm in areas dominated by quartz (Figures 1b, S3 - S5). Within relatively planar quartz ribbons, several crystals wide, the mean grain size is 47 (± 25) μm . Quartz grains are mostly equant, show a range of microstructures including undulatory and straight extinction, minor sub-grains, and both straight and irregular grain boundaries. Measurements obtained by EBSD from the quartz ribbons show a well developed crystallographic preferred orientation (CPO; M-index: 0.108; Figure 1b). Feldspar porphyroclasts range in size up to 5 mm, and are pervasively fractured (Figures 1b and S5). Feldspars are also present as < 20 μm neoblasts (10% of feldspars) that occur mainly in feldspar porphyroclast pressure shadows, where it is also associated with quartz neoblasts (Figures 1b and 2a). The feldspars are pure orthoclase and albite, with the orthoclase neoblasts having the same composition as the porphyroclasts (Figure S2). The neoblasts show a low degree of internal strain with misorientations generally < 1° (Figure 2b). Both quartz and feldspar (Figure 2c) neoblasts have a random CPO. The misorientation angle distribution plots for the feldspars approach the theoretical curve for random distributions (Figure 2d).

The mineralogy is much the same in the mylonite as in the protomylonite; however, phyllosilicates are more abundant and make up 20% of the rock, whereas feldspars,

in approximately equal proportions of K-feldspar and plagioclase, are less abundant at 45%. The bulk of the mylonite is made up of a fine-grained ($< 20 \mu\text{m}$), foliated mix of quartz, feldspars and phyllosilicates. The fine mixture is microstructurally and compositionally comparable to that formed in the porphyroclast pressure shadows in the protomylonite. A further portion of the phyllosilicates are arranged into interconnected layers a few grains thick (Figures 1c and 1d). Approximately 50% of the quartz occur in discontinuous ribbons a few grains wide, with a mean grain size of $29 (\pm 16) \mu\text{m}$ (excluding grains bordering the ribbon margins; Figures 1c, S3 and S4). Pole figures for quartz in these ribbons show well developed CPOs (M-index: 0.305; Figure 1c). Feldspar porphyroclasts are smaller and more rounded than in the protomylonite, with a median diameter of $500 \mu\text{m}$ and maximum grain size of 2 mm (Figure 1c). Porphyroclasts make up $\sim 50\%$ of the mylonite feldspar content, and are less fractured than in the protomylonite.

In the ultramylonites, the relative phase proportions are the same as in the mylonite. However, feldspar porphyroclasts, interconnected phyllosilicate layers and quartz ribbons are absent, and all constituent minerals are approximately uniformly distributed in an ultramylonitic mixture ($< 20 \mu\text{m}$) with the same grain size, shape and composition as the fine-grained mixtures observed locally in the protomylonite and mylonite (Figures 1e and 2e). The phyllosilicate sheet long axes are aligned to define the foliation in the ultramylonite, however, they are not interconnected (Figure 1e). Pole figures for quartz (M-index: 0.004; Figure 1e) and both feldspars (Figure 2g) in the ultramylonite show no distinct pattern, and misorientation angle distribution plots for feldspars similarly show a trend close to the theoretical curve of random distribution (Figure 2h). Furthermore, energy dispersive spectroscopy (EDS) maps show a uniform distribution of phases (Figure 2e), with similar low internal strain values (obtained by EBSD) as in the neoblast mixture in the protomylonite (Figure 2f).

4 Strain localisation mechanisms

The take-away message from the observations above is that the protomylonite, mylonite and ultramylonite all have distinct microstructures (Figures 3a and 3b). The protomylonite is coarse grained with fractured feldspar porphyroclasts and recrystallised quartz with a CPO. In the mylonite, phyllosilicates are arranged into interconnected layers that, along with dismembered quartz ribbons with a CPO, wrap around fractured feldspar por-

phyroclasts within an otherwise fine-grained matrix that lacks CPO. The ultramylonite is comprised of a uniformly distributed fine-grained mixture of all constituent phases that lacks both CPO and interconnected networks of weak phases.

In feldspar porphyroclasts the fractured nature and lack of dislocation creep microstructures imply that brittle deformation dominated with a likely frictional component (Figure 3b). Dissolution along their enveloping surfaces and new mineral growth also occurred, illustrated by neoblasts in pressure shadows (Figure 2a). The porphyroclasts and neoblasts have the same composition (Figure S2), as would be expected with brittle deformation and local dissolution precipitation. The rounded nature of feldspar porphyroclasts in mylonites could be attributed to crystal plasticity (Tullis & Yund, 1985). However, we do not observe evidence for crystal plastic deformation in feldspar, and rather suggest that the roundness is caused by precipitation creep and alteration reactions to muscovite and quartz (O'Hara, 1988). Quartz ribbons in the protomylonite and mylonite have developed CPOs (Figures 1b and 1c), as typical when deformed by dislocation creep (Law, 1990). Furthermore, in both the protomylonite and mylonite, quartz is found filling cracks in feldspar porphyroclasts (Figure S5), and as neoblasts precipitated in feldspar pressure shadows (Figures 1b, 1c and 2a). This mobility of components suggests diffusional processes were locally active. The arrangement of interconnected layers of phyllosilicates in the mylonites (Figures 1d and 3b), with low angles to shear zone boundaries, would have allowed for slip along grain boundaries and dislocation creep along the basal planes (Niemeijer & Spiers, 2005).

In the ultramylonites there are no fractured feldspar porphyroclasts, quartz dislocation creep microstructures, or interconnected phyllosilicate networks. A lack of CPO, the strain free nature of the grains, and misorientation angle distributions close to the theoretical random distribution curve all indicate that grain size sensitive creep was active during deformation (Wheeler et al., 2001; Menegon et al., 2015; Viegas et al., 2016). Pinning due to the polyphase nature of the rock would have kept the grain size small (Krabbendam et al., 2003; Herwegh & Berger, 2004; Kilian et al., 2011), in turn promoting diffusion creep and grain boundary sliding, accompanied by dissolution and precipitation processes (Fusseis et al., 2009; Platt, 2015; Menegon et al., 2015; Lopez-Sanchez & Llana-Fúnez, 2018).

5 Relative strengths in mylonites

Quartz paleopiezometry is commonly used to estimate stresses of naturally deformed rocks. In polyphase rocks, however, depending on the conditions of deformation and distribution of phases, the stress in quartz will either be higher or lower than the stress of the bulk rock. This is elegantly demonstrated in the KMZ, where quartz paleopiezometry on ribbon quartz, following closely the methods of Cross et al. (2017), yield higher stresses for the mylonite (54 MPa) than the protomylonite (39 MPa). We interpret the quartz as fully recrystallised and hence used the mean, without grain separation, of the full sample sets exhibiting unimodal grain size distributions (Figure S3), to obtain our stress estimates. As Cross et al. (2017) cautions, we acknowledge that great care is needed when applying paleopiezometry on quartz from natural mylonites deformed at the relatively high-grade metamorphic conditions (465 °C, 345 MPa) of the KMZ, where dislocation densities are low and grain boundary migration is likely the dominant mechanism with only minor sub-grain recrystallization. To correct for the paradox of higher stresses in the mylonite than the protomylonite, we used our microstructural observations in conjunction with Handy et al. (1999)'s equations, to obtain a strength estimate for the bulk rock (Text S1).

Feldspar is the strongest phase at the inferred conditions of deformation (465 °C, 345 MPa). The rocks will therefore have been relatively strong where feldspar locally forms a load-bearing framework (Handy et al., 1999). However, the feldspars are typically porphyroclasts, enveloped by quartz or a fine grained matrix. Most of the protomylonite will therefore have behaved according to Handy et al. (1999)'s frictional-viscous clastomylonite model, with strong, brittle feldspar (Byerlee, 1978; Jaeger & Cook, 1979) and relatively weak quartz deforming by dislocation creep (Hirth et al., 2001). As quartz in this case is the weaker of the two main strength determining phases, the stress estimated by quartz paleopiezometry is an underestimate for the bulk rock. The strain rate calculated for quartz is in turn an overestimate for the bulk rock, as it is greater in the quartz than in the stronger feldspar porphyroclasts. Following Handy et al. (1999), values of 67 MPa and $2.0 \times 10^{-13} \text{ s}^{-1}$ are obtained for the bulk rock stress and strain rate, respectively (Figure 3c).

In the mylonite, on the other hand, weak, interconnected networks of phyllosilicates, with flow strength best estimated using flow law parameters of Kronenberg et al. (1990),

are the dominant control on rock strength. Comparatively, quartz is now a stronger phase. As such, the stress (54 MPa) obtained by quartz paleopiezometry is an overestimate, and the strain rate of $1.5 \times 10^{-12} \text{ s}^{-1}$, calculated from the flow law of Hirth et al. (2001), is an underestimate for the bulk rock. Our calculations for the bulk rock mylonite give a differential stress of 33 MPa and strain rate of $3.3 \times 10^{-12} \text{ s}^{-1}$ (Figure 3c). Apart from being weaker than the protomylonite, these estimates are also similar to the maximum differential stress and strain rate calculated for a phyllosilicate bearing strike-slip fault at a depth of 14 km (30 MPa and 10^{-12} s^{-1} respectively; Niemeijer & Spiers, 2005).

As there are no ribbons in the ultramylonite, paleopiezometry can not be applied to estimate its strength. We can, however, assume a constant stress and/or strain rate and use the ranges obtained for the mylonite with Rybacki and Dresen (2000)'s diffusion creep flow law for feldspar. This results in differential stresses ranging from 2 to 127 MPa and strain rates from $1.6 \times 10^{-11} \text{ s}^{-1}$ to $1.0 \times 10^{-11} \text{ s}^{-1}$, if calculated with a fine grain size of $5 \mu\text{m}$ and the same P-T conditions as above (Figure 3c). Taking a grain size of $10 \mu\text{m}$ gives strengths higher than those in the mylonite. We note that the presence of grain boundary fluids will allow further weakening (McClay, 1977; Menegon et al., 2011). In other words, if the ultramylonite was monomineralic and consisted of fine-grained ($< 5 \mu\text{m}$) feldspar that deformed by wet diffusion creep, it is calculated to be slightly weaker than the mylonite. Separated by a narrow gradual contact (Figure 1a), the ultramylonite hosts much more localised strain than the mylonite, suggesting the ultramylonite was weaker. We therefore consider our calculations upper bounds for the strength of the polyphase mixture.

6 Implications for mid- to lower crustal strength

The transition from protomylonite to mylonite and eventually ultramylonite in the observed high strain zone is characterised by four distinct microstructural trends (Figures 1 and 3): 1) feldspar porphyroclasts becoming progressively smaller, rounder, and volumetrically less dominant; 2) an increasing percentage of an ultramylonitic fine-grained homogeneous mixture of all constituent phases; 3) the development and subsequent destruction of interconnected layers of phyllosilicates ; and 4) the development and destruction of a CPO in quartz.

The fine-grained mixture represents the ultramylonite shear zone core and the highest strains in the shear zone, implying that it is weaker than the interconnected phyllosilicate layers in the mylonite (Figure 3; cf. Handy, 1994; Montési, 2013). We therefore propose that as sufficient amounts of ultramylonitic mixture coalesce to form interconnected layers, it becomes the dominant control on bulk shear zone rheology. This transition coincides with dismemberment of the interconnected phyllosilicate layers, possibly by progressive flow of the weaker, fine-grained mixture or simply by thinning and extension of lithologic layering with progressive shear strain (Figure 3b; Cross & Skemer, 2017). Once the fine-grained mixture is formed, partly in the porphyroclast pressure shadows (Figures 2a and 3b), grain size sensitive deformation mechanisms will retain, sustain and maintain the weakness. The mixtures forming in feldspar porphyroclast pressure shadows, which themselves are smeared out along the foliation (Figures 1b and 1c), can therefore have an important role in the creation of highly localised ultramylonites.

Given the gradual nature of the microstructural variation in space (Figure 1a), we interpret progressive strain to have been the main driver in the evolution of the highly localised shear zone described above (Figure 3). This conforms with the experimentally derived time-dependent brittle-viscous transition put forward by Marti et al. (2017), in which grain size reduction of feldspar progressively changes the relative importance of brittle and viscous deformation in favour of the latter. Similarly, the KMZ provides a natural example for the experimental model of Cross and Skemer (2017) who proposed mechanical and geometric disaggregation during progressive shear strain as a mechanism for developing fine-grained ultramylonites (Figures 3b). Alternatively, highly localised shear zones, as described here but at smaller scale, have been associated with strain localisation within brittle precursors (Mancktelow & Pennacchioni, 2005). Similar weakening effects can also be created by stress driven strain localisation (Ellis & Stöckhert, 2004). For example, fine-grained mixtures could be obtained through creation and lithification of frictional melt along earthquake rupture planes in the mid-lower crust and be subsequently reactivated as ultramylonites (Menegon et al., 2017). We therefore acknowledge that shear zone cores comprised of fine grained mixtures do not imply a unique process, and highlight that a strain- and time dependent rheological evolution is simply our preferred interpretation of this exhumed example.

We emphasize that fine-grained mixtures in localised high strain zones, whichever way they are derived, are likely to control the long-term strength of quartzofeldspathic crust at temperatures in excess of the frictional-viscous transition in quartz. This conclusion is in accordance with recent proposals of weak, localised structures hosting post-seismic, accelerated deformation below the seismogenic zone (Ingleby & Wright, 2017). Attempts have been made at quantifying the rheological behaviour of polyphase rocks by combining single phase parameters (e.g. Platt, 2015; Ceccato et al., 2018); however, once grain size has reduced to favour grain size sensitive deformation mechanisms, the mixture may be weaker than any of its components (Wheeler, 1992). Thus, grain size can become more important than composition in controlling strain localisation, as suggested here for the KMZ (Figure 3). Although our observations were on quartzofeldspathic rocks deformed below the seismogenic zone, we note that recent experiments show that grain size sensitive creep may also lead to dynamic weakening during upper crustal earthquake propagation in carbonates (De Paola et al., 2015; Pozzi et al., 2019). From our study and several others (e.g. Rutter & Brodie, 1988; Warren & Hirth, 2006; Platt & Behr, 2011), it is therefore possible that strain localisation within fine-grained aggregates is important at a range of conditions and compositions throughout both continental and oceanic lithosphere.

7 Conclusions

Transitions from grain size insensitive creep to grain size sensitive creep have been widely recognised before (e.g. Fliervoet et al., 1997; Stünitz & Tullis, 2001; Kilian et al., 2011; Platt, 2015; Ceccato et al., 2018). However, our observations in the KMZ also show how a fine-grained polyphase mixture, deforming by grain size sensitive deformation mechanisms, is weaker than interconnected networks of phyllosilicates. Based on a gradual contact between mylonites and ultramylonites, and a preferred interpretation of a strain- and time dependent rheological evolution, we also suggest interconnected phyllosilicate networks may be broken down and supplanted by such fine-grained polyphase mixtures with increasing strain (Figure 3). This contradicts the common inference (e.g. Handy, 1994; Montési, 2013; Shea & Kronenberg, 1993) that interconnected layers of phyllosilicates represent the weakest state a shear zone can achieve and maintain, and emphasises the potential prevalence and importance of grain size sensitive creep as a fundamental control on lithospheric strength.

Acknowledgments

This project has received funding from the European Research Council under the Horizon 2020 programme (grant agreement No 715836 "MICA"). C.S. is funded by a Cardiff University College of Physical Sciences and Engineering Studentship. We thank D. Wilson at the University of Cape Town and A. Oldroyd at Cardiff University for sample preparation. L. Menegon provided invaluable discussion on EBSD analyses. The unwavering support of D. Muir at the Electron microbeam facility at Cardiff University is gratefully acknowledged. A. Kronenberg, V. Toy, B. Verberne and an anonymous reviewer provided constructive reviews that have significantly improved the manuscript. The EBSD data underpinning the results presented here can be accessed from the Cardiff University data catalogue at <http://doi.org/10.17035/d.2019.0076748607>.

References

- Bürgmann, R., & Dresen, G. (2008). Rheology of the lower crust and upper mantle: Evidence from rock mechanics, geodesy, and field observations. *Annual Review of Earth and Planetary Sciences*, *36*.
- Byerlee, J. (1978). Friction of rocks. *Pure and Applied Geophysics*, *116*, 615–626.
- Carreras, J. (2001). Zooming on Northern Cap de Creus shear zones. *Journal of Structural Geology*, *23*(9), 1457–1486.
- Ceccato, A., Menegon, L., Pennacchioni, G., & Morales, L. F. G. (2018). Myrmekite and strain weakening in granitoid mylonites. *Solid Earth*, *9*(6), 1399–1419.
- Cross, A., Prior, D., Stipp, M., & Kidder, S. (2017). The recrystallized grain size piezometer for quartz: An EBSD-based calibration. *Geophysical Research Letters*, *44*(13), 6667–6674.
- Cross, A., & Skemer, P. (2017). Ultramytonite generation via phase mixing in high-strain experiments. *Journal of Geophysical Research: Solid Earth*, *122*(3), 1744–1759.
- Czaplińska, D., Piazzolo, S., & Zibra, I. (2015). The influence of phase and grain size distribution on the dynamics of strain localization in polymineralic rocks. *Journal of Structural Geology*, *72*, 15–32.
- De Paola, N., Holdsworth, R. E., Viti, C., Collettini, C., & Bullock, R. (2015). Can grain size sensitive flow lubricate faults during the initial stages of earthquake propagation? *Earth and Planetary Science Letters*, *431*, 48–58.

- Diener, J. F., Fagereng, Å., & Thomas, S. A. (2016). Mid-crustal shear zone development under retrograde conditions: pressure–temperature–fluid constraints from the Kuckaus Mylonite Zone, Namibia. *Solid Earth*, 7(5), 1331–1347.
- Diener, J. F., White, R. W., Link, K., Dreyer, T. S., & Moodley, A. (2013). Clockwise, low-P metamorphism of the Aus granulite terrain, southern Namibia, during the Mesoproterozoic Namaqua Orogeny. *Precambrian Research*, 224, 629–652.
- Ellis, S., & Stöckhert, B. (2004). Elevated stresses and creep rates beneath the brittle-ductile transition caused by seismic faulting in the upper crust. *Journal of Geophysical Research: Solid Earth*, 109(B5).
- Fagereng, Å., & Biggs, J. (2018). New perspectives on 'geological strain rates' calculated from both naturally deformed and actively deforming rocks. *Journal of Structural Geology*.
- Fliervoet, T. F., White, S. H., & Drury, M. R. (1997). Evidence for dominant grain-boundary sliding deformation in greenschist-and amphibolite-grade polyminer-eralic ultramylonites from the Redbank Deformed Zone, Central Australia. *Journal of Structural Geology*, 19(12), 1495–1520.
- Fusseis, F., Regenauer-Lieb, K., Liu, J., Hough, R., & De Carlo, F. (2009). Creep cavitation can establish a dynamic granular fluid pump in ductile shear zones. *Nature*, 459(7249), 974–977.
- Handy, M. (1994). Flow laws for rocks containing two non-linear viscous phases: a phenomenological approach. *Journal of Structural Geology*, 16(3), 287–301.
- Handy, M., Wissing, S., & Streit, L. (1999). Frictional–viscous flow in mylonite with varied biminer-eralic composition and its effect on lithospheric strength. *Tectonophysics*, 303(1), 175–191.
- Herwegh, M., & Berger, A. (2004). Deformation mechanisms in second-phase af-fected microstructures and their energy balance. *Journal of structural geology*, 26(8), 1483–1498.
- Hirth, G., Teyssier, C., & Dunlap, J. W. (2001). An evaluation of quartzite flow laws based on comparisons between experimentally and naturally deformed rocks. *International Journal of Earth Sciences*, 90(1), 77–87.
- Hunter, N. J., Hasalová, P., Weinberg, R. F., & Wilson, C. J. (2016). Fabric controls on strain accommodation in naturally deformed mylonites: The influence of

- interconnected micaceous layers. *Journal of Structural Geology*, *83*, 180–193.
- Ingleby, T., & Wright, T. (2017). Omori-like decay of postseismic velocities following continental earthquakes. *Geophysical Research Letters*, *44*(7), 3119–3130.
- Jackson, M. P. A. (1976). High-grade metamorphism and migmatization of the Namaqua Metamorphic Complex around Aus in the southern Namib Desert, South West Africa. *Ph.D., University of Cape Town*.
- Jaeger, J. C., & Cook, N. G. W. (1979). *Fundamentals of rock mechanics* (3rd ed.). London: Chapman & Hall.
- Kilian, R., Heilbronner, R., & Stünitz, H. (2011). Quartz grain size reduction in a granitoid rock and the transition from dislocation to diffusion creep. *Journal of Structural Geology*, *33*(8), 1265–1284.
- Kirby, S. H. (1985). Rock mechanics observations pertinent to the rheology of the continental lithosphere and the localization of strain along shear zones. *Tectonophysics*, *119*(1-4), 1–27.
- Knipe, R. (1989). Deformation mechanisms - recognition from natural tectonites. *Journal of Structural Geology*, *11*(1-2), 127–146.
- Kohlstedt, D., Evans, B., & Mackwell, S. (1995). Strength of the lithosphere: Constraints imposed by laboratory experiments. *Journal of Geophysical Research: Solid Earth*, *100*(B9), 17587–17602.
- Krabbendam, M., Urai, J. L., & van Vliet, L. J. (2003). Grain size stabilisation by dispersed graphite in a high-grade quartz mylonite: an example from Naxos (Greece). *Journal of Structural Geology*, *25*(6), 855–866.
- Kronenberg, A. K., Kirby, S. H., & Pinkston, J. (1990). Basal slip and mechanical anisotropy of biotite. *Journal of Geophysical Research: Solid Earth*, *95*(B12), 19257–19278.
- Law, R. (1990). Crystallographic fabrics: a selective review of their applications to research in structural geology. *Geological Society, London, Special Publications*, *54*(1), 335–352.
- Lopez-Sanchez, M. A., & Llana-Fúnez, S. (2018). A cavitation-seal mechanism for ultramylonite formation in quartzofeldspathic rocks within the semi-brittle field (Vivero fault, NW Spain). *Tectonophysics*.
- Mancktelow, N. S., & Pennacchioni, G. (2005). The control of precursor brittle fracture and fluid–rock interaction on the development of single and paired ductile

- shear zones. *Journal of Structural Geology*, *27*(4), 645–661.
- Marti, S., Stünitz, H., Heilbronner, R., Plümper, O., & Drury, M. (2017). Experimental investigation of the brittle-viscous transition in mafic rocks—interplay between fracturing, reaction, and viscous deformation. *Journal of Structural Geology*, *105*, 62–79.
- McClay, K. (1977). Pressure solution and Coble creep in rocks and minerals: a review. *Journal of the Geological Society*, *134*(1), 57–70.
- Menegon, L., Fousseis, F., Stünitz, H., & Xiao, X. (2015). Creep cavitation bands control porosity and fluid flow in lower crustal shear zones. *Geology*, *43*(3), 227–230.
- Menegon, L., Nasipuri, P., Stünitz, H., Behrens, H., & Ravna, E. (2011). Dry and strong quartz during deformation of the lower crust in the presence of melt. *Journal of Geophysical Research: Solid Earth*, *116*(B10).
- Menegon, L., Pennacchioni, G., Malaspina, N., Harris, K., & Wood, E. (2017). Earthquakes as precursors of ductile shear zones in the dry and strong lower crust. *Geochemistry, Geophysics, Geosystems*.
- Miller, R., & Becker, T. (2008). The Geology of Namibia, vol. 2. *Geological Survey of Namibia, Windhoek*.
- Montési, L. G. (2013). Fabric development as the key for forming ductile shear zones and enabling plate tectonics. *Journal of Structural Geology*, *50*, 254–266.
- Niemeijer, A., & Spiers, C. (2005). Influence of phyllosilicates on fault strength in the brittle-ductile transition: Insights from rock analogue experiments. *Geological Society, London, Special Publications*, *245*(1), 303–327.
- O’Hara, K. (1988). Fluid flow and volume loss during mylonitization: an origin for phyllonite in an overthrust setting, North Carolina USA. *Tectonophysics*, *156*(1-2), 21–36.
- Platt, J. (2015). Rheology of two-phase systems: A microphysical and observational approach. *Journal of Structural Geology*, *77*, 213–227.
- Platt, J., & Behr, W. (2011). Grainsize evolution in ductile shear zones: Implications for strain localization and the strength of the lithosphere. *Journal of Structural Geology*, *33*(4), 537–550.
- Pozzi, G., De Paola, N., Holdsworth, R. E., Bowen, L., Nielsen, S. B., & Dempsey, E. D. (2019). Coseismic ultramylonites: An investigation of nanoscale viscous

- flow and fault weakening during seismic slip. *Earth and Planetary Science Letters*, 516, 164–175.
- Rennie, S., Fagereng, Å., & Diener, J. (2013). Strain distribution within a km-scale, mid-crustal shear zone: the Kuckaus Mylonite Zone, Namibia. *Journal of Structural Geology*, 56, 57–69.
- Rutter, E., & Brodie, K. (1988). The role of tectonic grain size reduction in the rheological stratification of the lithosphere. *Geologische Rundschau*, 77(1), 295–307.
- Rybacki, E., & Dresen, G. (2000). Dislocation and diffusion creep of synthetic anorthite aggregates. *Journal of Geophysical Research: Solid Earth*, 105(B11), 26017–26036.
- Shea, W. T., & Kronenberg, A. K. (1993). Strength and anisotropy of foliated rocks with varied mica contents. *Journal of Structural Geology*, 15(9-10), 1097–1121.
- Skemer, P., Katayama, I., Jiang, Z., & Karato, S.-i. (2005). The misorientation index: Development of a new method for calculating the strength of lattice-preferred orientation. *Tectonophysics*, 411(1-4), 157–167.
- Stünitz, H., & Tullis, J. (2001). Weakening and strain localization produced by syn-deformational reaction of plagioclase. *International Journal of Earth Sciences*, 90(1), 136–148.
- Tullis, J., & Yund, R. A. (1985). Dynamic recrystallization of feldspar: A mechanism for ductile shear zone formation. *Geology*, 13(4), 238–241.
- Viegas, G., Menegon, L., & Archanjo, C. (2016). Brittle grain-size reduction of feldspar, phase mixing and strain localization in granitoids at mid-crustal conditions (Pernambuco shear zone, NE Brazil). *Solid Earth*, 7(2), 375–396.
- Warren, J. M., & Hirth, G. (2006). Grain size sensitive deformation mechanisms in naturally deformed peridotites. *Earth and Planetary Science Letters*, 248(1), 438–450.
- Wheeler, J. (1992). Importance of pressure solution and Coble creep in the deformation of polymineralic rocks. *Journal of Geophysical Research: Solid Earth*, 97(B4), 4579–4586.
- Wheeler, J., Prior, D., Jiang, Z., Spiess, R., & Trimby, P. (2001). The petrological significance of misorientations between grains. *Contributions to Mineralogy and*

Petrology, 141(1), 109–124.

Figure 1. Images of rocks from the high strain zone marked in Figure S1. a: Looking down on mylonite (SW) - ultramylonite (NE) transition. b: Protomylonite (red box outlines location of Figures 2a and 2b). c: Mylonite. d: Interconnected layers of phyllosilicates from the same mylonite as c. e: Ultramylonite. All images display a dextral sense of motion and are oriented so the foliation is horizontal. b/c= cross-polarized optical micrographs, d/e= scanning electron microscope (SEM) backscattered electron images where quartz and albite are dark grey, K-feldspar is light grey and phyllosilicates are light grey and lamellar shape. Scales: a) coin= 22.6 mm; b/c) white bars=1 mm; d/e) white bars= 10 μm . Quartz c-axis plots are lower hemisphere equal area projections, Z= pole to foliation, X= lineation direction. Half width= 10° . n is the number of points used (one point per grain) and M stands for M-index (Skemer et al., 2005). Distances from the local shear zone core are indicated on b, c and e. Note same scale in d and e as well as the aligned and interconnected phyllosilicates in e compared to aligned but not interconnected phyllosilicates in d.

Figure 2. Electron backscatter diffraction (EBSD) analysis of porphyroclast pressure shadow marked in Figure 1b (left side: a/b/c/d) and ultramylonite (right side: e/f/g/h). a/e: EBSD band contrast image overlain by element maps derived by energy-dispersive X-ray spectroscopy (red=Si, blue=K, yellow=Na). b/f: Local misorientation maps. The maps show the degree of misorientation $\leq 3^\circ$ of each pixel with respect to the neighbouring pixels in a radius of 3x3 pixels. c/g: Pole figures with same reference frame as in Figure 1. d/h: Misorientation angle distribution plots.

Figure 3. Schematic illustration of the strain- and time-dependent rheological evolution of the studied shear zone. a) Representative microstructures for protomylonite, mylonite and ultramylonite, based on photomicrographs in Figure 1, with locations for areas of interest. b) Dominant deformation and dispersion mechanisms. c) Strength graph with both differential stress and strain rate estimates (see section on 'Relative strength of mylonites' for details) showing decreasing strength from protomylonite to mylonite and further to the ultramylonite. Star denotes peak strength estimate for a phyllosilicate bearing strike-slip fault such as the San Andreas (Niemeijer & Spiers, 2005).

Figure 1.

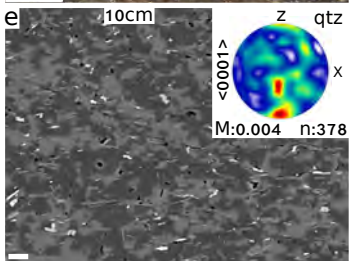
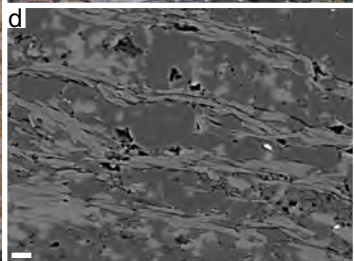
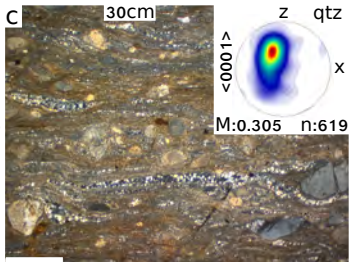
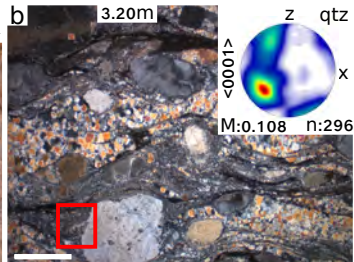
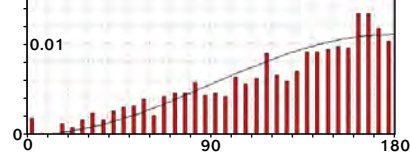
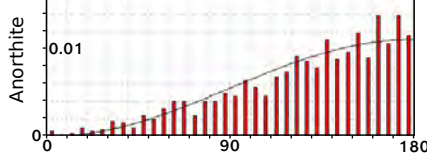
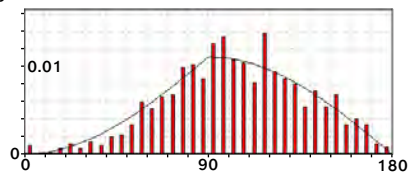
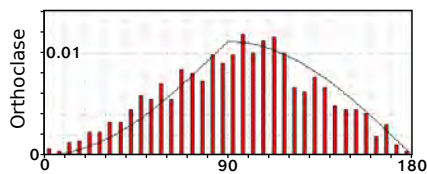
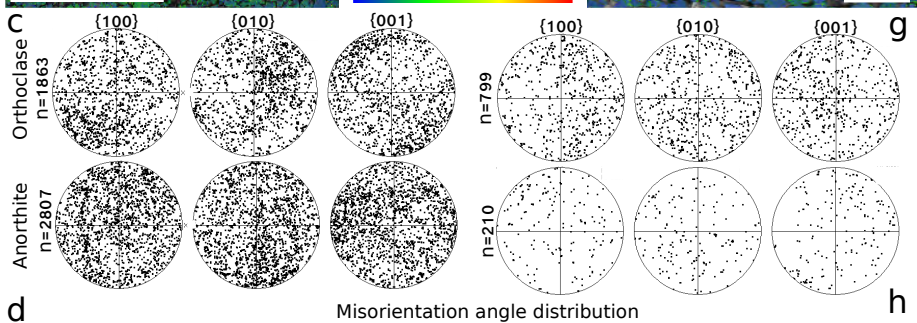
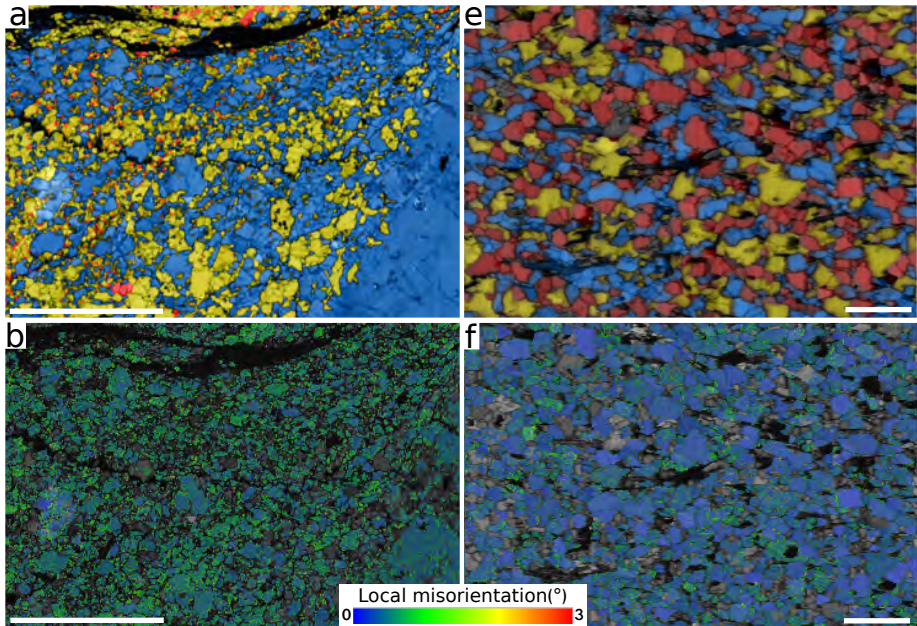


Figure 2.



■ Uncorrelated (1000) — Random (theoretical)

Figure 3.

